Plant Physiology and Biochemistry 135 (2019) 511–519

Contents lists available at ScienceDirect

Plant Physiology and Biochemistry

journal homepage: www.elsevier.com/locate/plaphy

Research article

Comparative "phenol-omics" and gene expression analyses in peach (*Prunus persica*) skin in response to different postharvest UV-B treatments

Marco Santin[a,c], Luigi Lucini[b], Antonella Castagna[a,*], Gabriele Rocchetti[b], Marie-Theres Hauser[c], Annamaria Ranieri[a,d]

[a] Department of Agriculture, Food and Environment, University of Pisa, via del Borghetto 80, 56124, Pisa, Italy
[b] Department for Sustainable Food Process, Università Cattolica del Sacro Cuore, Via Emilia Parmense, 84, 29122, Piacenza, Italy
[c] Department of Applied Genetics and Cell Biology, University of Natural Resources and Life Sciences, Muthgasse 18, 1190, Vienna, Austria
[d] Interdepartmental Research Center Nutrafood "Nutraceuticals and Food for Health", University of Pisa, Via del Borghetto 80, 56124, Pisa, Italy

ARTICLE INFO

Keywords:
Anthocyanins
Fruit
Phenylpropanoid biosynthesis
Secondary metabolites
UV radiation
UVR8

ABSTRACT

Ultraviolet-B (UV—B) radiation impacts the plant behaviour in many ways, including modifying their secondary metabolism. Although several studies have quantified the UV-B effects on phenolic composition, most of them focused on leaves or investigated a limited amount of phenolics. The present work aimed to investigate the phenolic changes after two postharvest UV-B treatments, 10 and 60 min (1.39 kJ m^{-2} and 8.33 kJ m^{-2}, respectively), on peach (*Prunus persica* cv Fairtime) fruit with a non-targeted, whole profiling approach, and targeted gene expression analysis on skin. After both UV-B exposures, peach fruit were harvested at 24 and 36 h for "phenol-omics" analysis, while additional 6 h and 12 h recovery times were used for gene expression analysis. Our results revealed that both UV-B exposures resulted in a decrease of several phenolic compounds, such as anthocyanins, after 24 h from the exposure. In contrast, the expression of the UV-B signalling components, the phenylpropanoid biosynthesis genes and their transcriptional regulators increased 6 h after the treatment, mostly with a UV-B-dose dependent behaviour, preceding an accumulation of most phenolics in both the UV-B treatments at 36 h compared to 24 h. Orthogonal projections to latent structures discriminant analysis (OPLS-DA) revealed that flavonoids, particularly anthocyanins, were the main phenolic subclasses accumulated after UV-B exposure.

1. Introduction

Sunlight is a crucial environmental factor for a wide range of aspects during plant development. Not all the ultraviolet (UV) wavelengths from the solar spectrum reach the Earth surface, since all the extremely harmful UV-C (100–280 nm) and most of the UV-B radiations (280–315 nm) are filtered by the stratospheric ozone layer. Although the Earth-reaching UV-B radiation is estimated to be less than 0.5%, it affects many biochemical, molecular and physiological processes in plants. Indeed, UV-B radiation has enough energy to cause damages to many cellular macromolecules, such as nucleic acids, proteins and membrane lipids, leading to potentially deadly effects for plants (Jenkins, 2014). However, since plants are sessile organisms and cannot escape the UV-B radiation, they have evolved effective responses in order to minimise the damages caused by UV-B (Frohnmeyer, 2003). Such acclimation responses are mainly related to an over-expression of genes involved in both DNA repair and the accumulation of UV-B screens and metabolites scavenging reactive oxidative species (ROS) such as phenylpropanoids and carotenoids (Zhang and Tian, 2009) (Zhang and Tian, 2009). The modulation in the transcript levels of several genes involved in UV-B acclimation are the result of a specific cellular pathway mediated by the UV-B photoreceptor called UV RESISTANCE LOCUS 8 (UVR8). Structurally, UVR8 is a homodimeric protein located in the cytosol (Rizzini et al., 2011). Once irradiated with

Abbreviations: 4CL, 4-COUMARATE:COA LIGASE; ANS, ANTHOCYANIDIN SYNTHASE; C4H, CINNAMATE 4-HYDROXYLASE; CHI, CHALCONE ISOMERASE; CHS, CHALCONE SYNTASE; COP1, CONSTITUTIVELY PHOTOMORPHOGENIC 1; DFR, DIHYDROFLAVONOL 4-REDUCTASE; EIF4A, EUKARYOTIC INITIATION FACTOR 4A; F3′H, FLAVONOID 3′—HYDROXYLASE; F3H, FLAVANONE 3-HYDROXYLASE; HY5, ELONGATED HYPOCOTYL 5; MYB, myeloblastosis; OPLS-DA, orthogonal projection to latent structures discriminant analysis; PAL, PHENYLALANINE AMMONIA-LYASE; ROS, reactive oxygen species; RUP, REPRESSOR OF UV-B PHOTOMORPHOGENESIS1; TUB9, tubulin beta-9 chain; UBQ5, ubiquitin 5; UFGluT, UDP-GLUCOSE:FLAVONOID 3-O-GLUCOSYLTRANSFERASE; UV, ultraviolet; UVR8, UV RESISTANCE LOCUS 8; VIP, variables importance in projection

* Corresponding author.
E-mail address: antonella.castagna@unipi.it (A. Castagna).

https://doi.org/10.1016/j.plaphy.2018.11.009
Received 28 August 2018; Received in revised form 6 November 2018; Accepted 8 November 2018
Available online 12 November 2018

UV-B, UVR8 protein undergoes conformational changes that convert the homodimer into two active monomers, which trigger a signalling pathway (Jenkins, 2014). Firstly, the UVR8 monomer interacts with CONSTITUTIVELY PHOTOMORPHOGENIC 1 (COP1), which is an E3 ubiquitin-ligase, preventing the degradation of ELONGATED HYPOCOTYL 5 (HY5) bZIP transcription factor (Favory et al., 2009). The UVR8-COP1 complex activates the transcription of target genes involved in UV-B acclimation, such as phenolic biosynthetic genes (Cloix et al., 2012; Rizzini et al., 2011). HY5 acts redundantly to promote the transcription of downstream genes (Favory et al., 2009). Brown et al. (2005) found that HY5 promotes the expression of several phenolic-related genes, which in turn are involved in UV-B acclimation. Induction of several flavonoid biosynthetic genes, such as *CHALCONE SYNTASE* (*CHS*), *CHALCONE ISOMERASE* (*CHI*), *FLAVANONE 3-HYDROXYLASE* (*F3H*), *DIHYDROFLAVONOL 4-REDUCTASE* (*DFR*), *ANTHOCYANIDIN SYNTHASE* (*ANS*), and *UDP-GLUCOSE:FLAVONOID 3-O-GLUCOSYLTRANSFERASE* (*UFGluT*) was detected in different fruit, like apple (Ubi et al., 2006) and tomato (Catola et al., 2017). Also in peach fruit, a study showed an increase in the expression of several flavonoid-related genes, such as *PpCHS*, *PpCHI*, *PpF3H* and *PpDFR* genes in specific peach cultivars (Suncrest and Big Top) after a 36 h UV-B treatment (Scattino et al., 2014). Most of flavonoid biosynthetic genes are regulated by a large transcription factor family, the V-myb myeloblastosis viral oncogene homolog (MYB), widely spread in all eukaryotes and especially within plants. The largest MYB group, R2R3-MYB, is related mainly to primary and secondary metabolism, defence against biotic and abiotic stresses and growth regulation (Falcone Ferreyra et al., 2012).

Polyphenols represent a wide class of secondary metabolites generally spread throughout the plant kingdom, which are responsible for the acclimation of plants towards adverse environmental conditions. Together with some vitamins and dietary fibres, polyphenols contribute to the well-known beneficial properties of plant-based food. Nowadays, rising consumers' demands of health-promoting products have led food companies and farm growers to search for new eco-friendly technologies that can provide a concrete increase of nutraceutical value in fruit and vegetable. Recent evidences have shown that UV-B radiation is able to modulate metabolic profile, promoting the accumulation of some polyphenolic compounds (Schreiner et al., 2014).

However, literature about effects of postharvest UV-B treatments in fruit is scanty. Few studies investigated the UVR8-mediated mechanism for UV-B perception in fruit, as well as which phenolic compounds are the mainly ones affected by UV-B radiation (Santin et al., 2018; Scattino et al., 2014). This work was aimed to determine a time course of UV-B stimulated transcription of genes involved in the UVR8 signalling, in the biosynthesis of phenolics and their transcriptional regulators, together with the quantification of phenolics with an "-omics" approach, in peach skin.

2. Materials and methods

2.1. Plant material and UV-B treatment

Organic peach fruit (*Prunus persica* L., cv Fairtime) were bought in an organic grocery store and immediately transported to the laboratory of the Department of Applied Genetics and Cell Biology at the University of Natural Resources and Life Sciences, Vienna (Austria). Undamaged fruit were selected to be comparable in color and dimensions (8.1 cm average diameter). Peach skin ranged from yellow to red (Fig. S1), thus individual fruit were accurately UV-B irradiated and sampled mostly on the yellow part. The peaches were all at the same ripening stage, which coincided with the commercial maturity.

Five peaches were rapidly sampled after arrival at the laboratory and represent time 0 (T_0). Remaining peaches were distributed equally to control and two separate UV-B treatments for 10 min and 60 min. UV-B treatments were conducted inside proper climatic chambers (24 °C), each supplied with four UV-B tubes (Philips Ultraviolet-B Narrowband, TL 20W/01 – RS, Koninklijke Philips Electronics, Eindhoven, The Netherlands). UV-B dose provided was 1.39 kJ m^{-2} and 8.33 kJ m^{-2} in the 10 min and 60 min UV-B treated groups at fruit height, respectively. Each chamber was also equipped with white light, reaching a total irradiance of 6.42 kJ m^{-2} and 38.53 kJ m^{-2} in the 10 min and 60 min groups at fruit height, respectively. The chamber for the control treatment had only white light. Skin tissue (less than 1 mm thick) of the UV-B exposed area was sampled after 6 h, 12 h, 24 h, and 36 h from the start of the UV-B irradiation with scalpel and tweezers, immediately frozen in liquid nitrogen followed by lyophilized and kept at −80 °C until analyses. Five peaches per treatment (control, UV-B 10 min and UV-B 60 min) were sampled at each time points mentioned. The skin collected from each fruit was kept separately, and therefore represents a biological replicate.

2.2. RNA isolation and cDNA synthesis

RNA was extracted from lyophilized skin samples using the LiCl/CTAB method, as described by Richter et al. (2017) with few modification. Briefly, 50 mg of lyophilized material were ground to fine powder and mixed with 3 mL of pre-heated RNA extraction buffer (2% [w/v] hexadecyltrimethylammonium bromide, CTAB; 2% [w/v] polyvinylpyrrolidone, PVP; 100 mM Tris/HCl pH 8.0; 25 mM EDTA; 2 M NaCl; 0.5 g/L spermidine and 2.7% [v/v] 2-mercaptoethanol). The suspension was incubated at 65 °C for 5 min. 3 mL of ice-cold chloroform:isoamylalcohol (24:1) were added and mixed for 5 min. After centrifugation (4250 g for 20 min at 4 °C), supernatant was transferred to a new tube and an additional washing step with ice-cold chloroform:isoamylalcohol (24:1) followed by centrifugation was performed. RNA was precipitated adding ice-cold 10 M LiCl at 4 °C overnight. After centrifugation (12000 g for 1 h at 4 °C), the RNA pellet was washed with 75% EtOH, resuspended in 30 μL RNAse free water and stored at −80 °C. RNA quantification was performed using Qubit (Invitrogen) and the NanoDrop systems. To control the integrity of the isolated RNA 1 μL was separated on a 1.2% agarose gel. To remove genomic DNA traces, RNA was treated with 1 U RNase-free DNaseI (Fermentas) in the presence of 25 mM $MgCl_2$ at 37 °C for 30 min, as stated by Karsai et al. (2002). RNA was reverse transcribed in 15 μL using 1 μL of peqGOLD M-MuLV H Plus, 200 U/μL (Peqlab), in a RT master mix containing 5 × RT buffer (provided with RT enzyme), 1 mM dNTP and 50 pMol oligo (dT)18. Samples were kept at 37 °C for 60 min, then the reaction was stopped by incubation at 75 °C for 5 min. Resulting cDNA was diluted 5 times with sterile double-distilled water, and stored at −20 °C.

2.3. Real time quantitative PCR (RT-qPCR)

PpEIF4A (*EUKARYOTIC INITIATION FACTOR 4A*) was found to be the most stable gene among three reference genes candidates tested (*PpEIF4A*, TUBULIN BETA-9 CHAIN (*PpTUB9*) and UBIQUITIN 5 (*PpUBQ5*)), therefore was used to normalize the RT-qPCR data of all the genes. Primers for *PpEIF4A*, *PpCHS*, *PpF3H*, *PpF3′H*, *PpDFR*, *PpMYB111*, *PpMYB-like*, *PpCOP1*, *PpHY5*, *PpUVR8* were designed based on the latest GenBank database and the Genome Database for Peach *Prunus persica* genome (https://www.rosaceae.org/species/prunus_persica/genome_v2.0.a1) and homology searches with BLAST (Altschul et al., 1997), using the *Arabidopsis* genes as starting point. Sequences are reported in tblS1was performed using a Rotorgene-3000 cycler (Corbett, Qiagen, Germany) and the 5× HOT FIREPol EvaGreen® qPCR Mix Plus (Solis BioDyne, Tartu, Estonia). Each reaction was done in triplicate. RT-qPCR reaction was performed in a total volume of 14 μL, consisting in 2.8 μL of 5× HOT FIREPol EvaGreen® qPCR Mix, 0.25 μL of forward and reverse primers (20 μM), 1 μL of the cDNA template, and double-distilled water. After an initial denaturation step (95 °C/12 min), amplification was done with 40 cycles as follows: 55 °C/5 s, 67 °C/25 s (extension and acquisition in channel A), 76 °C/6 s (acquisition in channel B), 82 °C/6 s

(acquisition in channel C) and denaturation at 95 °C/5 s. For each gene, a standard curve of serial diluted templates (from 10^7 to 10^2, with 10^5, 10^4 and 10^3 in duplicate, and a blank) was created to calculate the PCR efficiency (Table S1). A standard curve was also included in each RT-qPCR reaction. Quantification in terms of number of copies/μL was performed with RotorGene software system using the gene specific standard curves, and results were normalised with respect to the *PpEIF4A* reference gene copy number. For each gene, standard curves of known PCR amplicon copy number were designed, and serial dilutions of quantified PCR fragment were included in each run and the PCR efficiencies determined. RT-qPCR data represent means and standard errors of five independent biological replicates.

2.4. Extraction and UHPLC-ESI-QTOF-MS screening of phenolic compounds

Five individual replicates from each sample were extracted in 10 mL of 0.1% formic acid in a methanol (LC-MS grade, VWR, Milan, Italy) and water mixture (80/20, v/v) for 5 min using an Ultra-turrax (Ika T25, Staufen, Germany). The extracts were centrifuged at 6000 × *g* for 10 min at 4 °C and the resulting solutions filtered using 0.22 μm cellulose syringe filters into amber vials for further use. Phenolic compounds were then screened in peach skin by means of an untargeted ultra-high-performance liquid chromatography (UHPLC) coupled to a quadrupole-time-of-flight high-resolution mass spectrometer via an electrospray ionization system (UHPLC-ESI-QTOF-MS). The analytical conditions for the analysis of phenolic compounds in this matrix were optimized in previous experiments (Santin et al., 2018). Briefly, the mass spectrometer worked in positive SCAN mode, in order to acquire metabolites in the range 100–1200 m/z. Raw data were analyzed using the Agilent Profinder B.06 software (Agilent technologies, Santa Clara, CA, USA) and considering the 'find-by-formula' algorithm. The high confidence in identification was recursively reached by coupling accurate mass together with isotope pattern (isotopic spacing and ratio). Features that were not present in 100% of replications within at least one treatment were not considered. The database exported Phenol-Explorer 3.6 (Rothwell et al., 2013) was used as reference in the identification, adopting a 5-ppm tolerance for mass accuracy.

After that, considering the availability of nine phenolic standards, polyphenols identified were also quantified according to their corresponding phenolic subclasses. In particular, five concentrations over five orders of magnitude for each methanolic standard solutions were injected into UHPLC/QTOF to achieve this goal. Cyanidin (2-(3,4-Dihydroxyphenyl) chromenylium-3,5,7-triol; anthocyanins), (+)-catechin (flavanols), luteolin (3′,4′,5,7-Tetrahydroxyflavone; flavones and other remaining flavonoids), resveratrol (3,4′,5-Trihydroxy-trans-stilbene; stilbenes), 5-pentadecylresorcinol (alkylphenols), tyrosol (tyrosols and other remaining low molecular weight phenolics), ferulic acid (trans-ferulic acid; hydroxycinnamics acids and other phenolic acids), sesamin (furofuran lignans) and matairesinol (dibenzylbutyrolactone and dihydroxydibenzylbutane lignans) were considered as representative of their respective phenolic class. All standard compounds were purchased from Extrasynthese (Genay, France) each having a purity > 98%. Calibration curves were built using a linear fitting (unweighted and not forced to axis-origin) in the range 0.05–500 mg L^{-1}; a coefficient of determination $R^2 > 0.97$ was used as acceptability threshold for calibration purposes.

2.5. Statistical analysis

JMP software (SAS Institute, Inc., Cary, NC) was used for statistical analysis. The effect of UV-B treatment on gene expression, total phenolics, anthocyanins, hydroxycinnamic acids and flavonols considering separately each recovery time point, was evaluated with one-way ANOVA followed by Tukey–Kramer post hoc test at the significance level $P \leq 0.05$.

Metabolomic data on the phenolic profile observed considering both UV-B treatment (0-10-60 min) and recovering time (24–36 h) were elaborated using the software Agilent Mass Profiler Professional B.12.06. In particular, all phenolic compounds identified were filtered by abundance and by frequency, normalised at the 75th percentile and baselined to the corresponding median in all samples. Afterwards, the metabolomics-based dataset was exported into the software SIMCA 13 (Umetrics, Malmo, Sweden), UV scaled and elaborated by means of orthogonal projection to latent structures discriminant analysis (OPLS-DA) supervised modelling (Rocchetti et al., 2018). The variation between groups was taken into account considering both predictive and orthogonal components. The presence of outliers in the model was also evaluated according to Hotelling's T2, using 95% and 99% confidence limits for suspect and strong outliers, respectively. The discriminant model was cross-validated using CV-ANOVA ($p < 0.01$) and permutation testing ($N = 100$) applied to exclude model overfitting. The goodness-of-fit (R^2Y) and the goodness-of-prediction (Q^2Y) of the model were also taken into account. Besides, the variables importance in projection (VIP) approach was used to identify the best marker of the phenolic profiles observed, *i.e.* those better able to discriminate the different samples. To this aim, phenolic compounds having a VIP score > 1 were exported. Finally, the contribution plot, considering both 10 min UV-B treated samples (24 *vs* 36 h) and 60 min UV-B treated samples (24 *vs* 36 h), was used to highlight which variables participated in the observed fold-change distribution.

3. Results and discussion

3.1. Effect of UV-B treatment on the comprehensive phenolic profile of peach skin

Phenolic compounds are considered very strong absorbers of the UV-B radiation and their accumulation into the fruit could be the direct consequence of UV-B eliciting effects, as pointed out in previous literature (Scattino et al., 2014). However, to date, few works (Santin et al., 2018) focused the attention on the comprehensive change of the phenolic profile after different UV-B treatments. In this study, the UHPLC-ESI-QTOF-MS system followed by the compounds identification through Phenol-Explorer 3.6 database provided an accurate method for elucidating the phenolics within skin peach samples. A multivariate statistic was used to explain the different phenolic profile observed when considering both the recovering time (i.e., 24 and 36 h) and the UV-B treatment type (0-10-60 min). More than 200 phenolic compounds have been detected, highlighting a high level of complexity (Tab. S2). The main phenolics present in peach skin were flavonols, hydroxycinnamic acids, tyrosols and anthocyanins, which together constituted around half of all the phenols identified.

Although not significantly, the 60 min-UV−B-treatment determined a 16% decrease in total phenolics after 24 h (Table 1), followed by a 23% increase after 36 h compared to the 60 min UV-B treated after 24 h. Such trend was particularly observed for anthocyanins, which were significantly reduced after both UV-B treatments at 24 h, but then they increased significantly after 36 h. No changes were detected in hydroxycinnamic acids and flavonols concentration in both the 10 min and 60 min UV-B-treated samples.

Furthermore, UV-B treatment induced the accumulation of a greater variety of anthocyanins, which were visible after 36 h from the UV-B exposure (Tab. S2). In fact, a newly-synthesized anthocyanin appeared after 36 h, the delphinidin, together with several more differentially glycosylated anthocyanins already present after 24 h, especially regarding the cyanidin.

Multivariate statistical analysis of high-throughput metabolomics data is usually performed by means of supervised (i.e., PLS-DA or OPLS-DA) and unsupervised (i.e., hierarchical cluster analysis or PCA) approaches. PLS-DA is usually performed for classification purposes in order to consider those variables that maximize the discrimination

Table 1
Total phenolics, anthocyanins, hydroxycinnamic acids and flavonols (mg/kg d.w.) detected in skin of peach fruit irradiated with 10 min and 60 min UV-B (1.39 kJ m^{-2} and 8.33 kJ m^{-2}, respectively).

Sampling time after UV-B exposure	UV-B exposure time	Total phenolics	Anthocyanins	Hydroxycinnamic acids	Flavonols
24 h					
	0 min	838 ± 54	102 ± 17[a] (12%)	145 ± 20 (17%)	184 ± 19 (22%)
	10 min	818 ± 73	43 ± 7[b] (5%)	160 ± 19 (20%)	189 ± 28 (23%)
	60 min	700 ± 32	57 ± 6[b] (8%)	104 ± 15 (15%)	176 ± 22 (25%)
36 h					
	0 min	834 ± 17	35 ± 8[b] (4%)	168 ± 17 (20%)	212 ± 12 (25%)
	10 min	802 ± 41	59 ± 11[ab] (7%)	168 ± 10 (21%)	196 ± 19 (24%)
	60 min	860 ± 66	85 ± 14[a] (10%)	100 ± 28 (12%)	226 ± 16 (26%)

Percentages for each phenolic subclass on the total phenolics are given in brackets. Data are mean ± SE of five biological replicates. Different letters correspond to statistically significant differences according to one-way ANOVA followed by Tukey–Kramer post hoc test ($P \leq 0.05$).

between sample groups or even to predict class affiliations of unclassified samples based on a calibration set of known class distributions (Bartel et al., 2013). However, the variation not directly correlated with Y is still present in the final scores, complicating the interpretation of PLS-DA results with a high number of classes (Worley and Powers, 2013). Therefore, in this work, the OPLS-DA model was used to effectively separate Y-predictive variation from Y-uncorrelated variation in X (i.e., orthogonal signal).

The discriminant model based on phenolic profile was found to be very robust, showing more than acceptable diagnostic and cross-validation parameters. Particularly, the goodness-of-fit (R^2Y) and the goodness-of-prediction (Q^2Y) were 0.91 and 0.61, respectively, with adequate CV-ANOVA and permutation test cross-validation. In fact, no outliers were recorded when considering the 95% and 99% confidence limits, as assessed by the Hotelling's T2 Range (Fig. S2). The absence of overlapping in the model was confirmed by means of dedicated statistical experiments (Tab. S3, Tab. S4). The OPLS-DA allowed to figure out the behaviour of all the phenolics with an -omics approach. The output of the OPLS-DA score plot considering each group of peach fruit extracts is provided as Fig. 1. The first component of the OPLS-DA score plot provided a clear separation between the 24 h group (located in the negative half of the plot) and the 36 h (located in the positive half of the plot), suggesting a completely different phenolic profile in the skin sampled after 24 or 36 h. Another interesting result was highlighted by the second component of the OPLS-DA score plot. In fact, samples belonging to the recovery time 24 h showed a different positioning into the score plot when considering the control (0 min) and the UV-B treated samples (10 and 60 min), indicating variation in the phenolic pattern. A different grouping was obtained when considering the 36-h recovery group, being the samples very closed into the space, suggesting a very similar phenolic profile. The control samples simply moved along the first component, indicating a possible change in the phenolic profile due only to the physiological maturation of the fruit.

The differential trends observed into the OPLS-DA score plot for the 24-h recovering time might be related, as already hypothesized, to the decrease of phenolic compounds, after both 10 and 60 min of UV-B treatment, trying to counteract the potentially disruptive effects of UV-B radiation (Santin et al., 2018). Therefore, from our results, it appears evident that the recovering time (24 h vs 36 h) was the most discriminant factor when compared to the extent of the UV-B treatment (10 vs 60 min), thus determining a general change of the phenolic composition.

Considering that the main differences were represented into the metabolomic dataset, the 'variable of importance' (VIP) approach was carried out in order to describe which phenolic compound possessed the highest discrimination potential into the OPLS-DA model. Table 2 reported the 36 phenolic markers with the highest VIP scores (> 1), classified considering both class and phenolic subclass. Overall, the most abundant phenolics belonged to flavonoids (19 compounds), anthocyanins and flavonols being the most represented subclasses. Interestingly, glycosidic forms of cyanidin possessed some of the highest VIP scores, being 1.33, 1.17 and 1.16, thus confirming their involvement into the modulation of the phenolic profile observed over time as a consequence of the UV-B treatment. Importance of anthocyanins as UV-B protectants was recently observed in other studies, which showed that anthocyanins were the most up-regulated subclass of phenolics after a

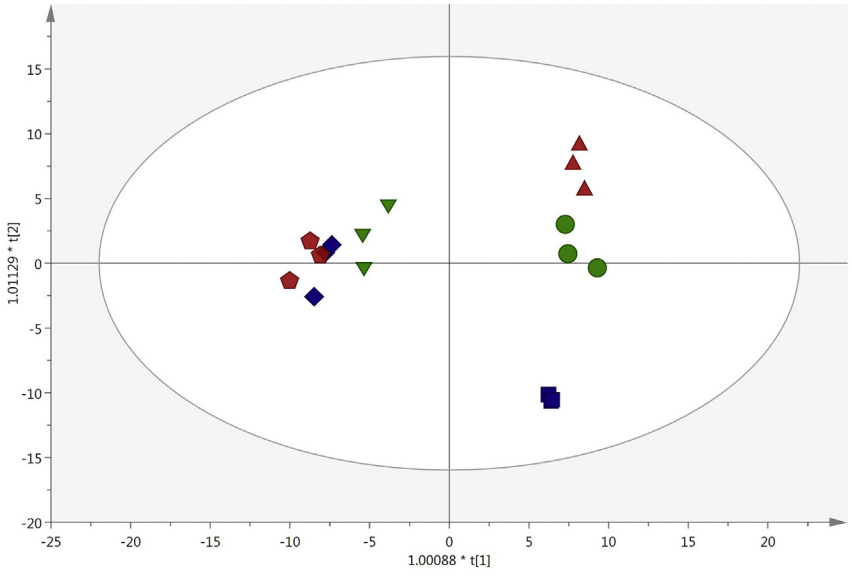

Fig. 1. Orthogonal Projection to Latent Structures Discriminant Analysis (OPLS-DA) carried out from the UHPLC-ESI-QTOF phenolic profile in the samples investigated, considering both UV-B treatment (0-10-60 min, 0 kJ m^{-2}, 1.39 kJ m^{-2} and 8.33 kJ m^{-2} UV-B, respectively) and recovery time (24 vs 36 h). Individual replications are given in the class prediction model score plot.

Table 2
Discriminant phenolics identified according to VIP (Variable Importance in Projection) following OPLS-DA.

Phenolic class	Phenolic subclass	Marker	VIP score
Flavonoids	Anthocyanins	Cyanidin 3-*O*-(6''-*p*-coumaroyl-glucoside)	1.33 ± 0.41
		Cyanidin 3-*O*-(6''-acetyl-galactoside)	1.17 ± 0.50
		Cyanidin 3-*O*-galactoside	1.16 ± 0.51
		Pelargonidin 3-*O*-rutinoside	1.09 ± 0.29
		Petunidin 3-*O*-galactoside	1.07 ± 0.41
		Petunidin 3-*O*-(6''-*p*-coumaroyl-glucoside)	1.06 ± 0.38
		Vitisin A	1.03 ± 0.34
	Dihydrochalcones	Phloretin 2′−*O*-xylosyl-glucoside	1.12 ± 0.41
	Flavanols	Catechin 3-*O*-gallate	1.04 ± 0.35
	Flavanones	Naringin 4′−*O*-glucoside	1.13 ± 0.23
	Flavones	Luteolin 7-*O*-(2-apiosyl-6-malonyl) -glucoside	1.10 ± 0.15
		Isorhoifolin	1.09 ± 0.17
		Cirsilineol	1.07 ± 0.24
	Flavonols	Quercetin	1.21 ± 0.23
		Rhamnetin	1.05 ± 0.26
		Kaempferol 3-*O*-(2''-rhamnosyl-6''-acetyl-galactoside) 7-*O*-rhamnoside	1.04 ± 0.23
		Quercetin 7,4′−*O*-diglucoside	1.03 ± 0.23
		3,7-Dimethylquercetin	1.02 ± 0.14
	Isoflavonoids	6''−*O*-Acetylglycitin	1.03 ± 0.31
Lignans	–	Cyclolariciresinol	1.15 ± 0.31
		7-Oxomatairesinol	1.07 ± 0.27
		Sesaminol	1.03 ± 0.33
		Secoisolariciresinol-sesquilignan	1.03 ± 0.20
		Sesamin	1.02 ± 0.10
Phenolic acids	Hydroxycinnamics	Cinnamic acid	1.30 ± 0.39
		3-*p*-Coumaroylquinic acid	1.13 ± 0.26
		Feruloyl glucose	1.13 ± 0.26
		Sinapic acid	1.10 ± 0.21
Other polyphenols	Alkylphenols	5-Pentadecylresorcinol	1.02 ± 0.11
	Curcuminoids	Bisdemethoxycurcumin	1.07 ± 0.26
	Furanocoumarins	Isopimpinellin	1.16 ± 0.23
	Hydroxybenzaldehydes	Vanillin	1.10 ± 0.29
	Hydroxybenzoketones	3-Methoxyacetophenone	1.09 ± 0.16
	Hydroxycoumarins	Mellein	1.15 ± 0.28
	Others	Catechol	1.19 ± 0.26
		3,4-Dihydroxyphenylglycol	1.14 ± 0.31

Compounds are provided together with VIP scores (measure of variables' importance in the OPLS-DA model).

postharvest UV-B treatment on apples (Assumpção et al., 2018). As regard the other phenolic markers, high VIP scores were recorded for cinnamic acid (hydroxycinnamic acid), quercetin (flavonol), cyclolariciresinol (lignan) and lower-molecular-weight phenolics (i.e., mellein, catechol and isompimpinellin).

3.2. Fold-change analysis on phenolic compounds

A fold-change analysis was performed using the UHPLC-ESI-QTOF-MS data on all the phenolics detected, and a fold-change graph was built for each UV-B treatment (10 min and 60 min), considering the 36 h against the 24 h recovery time points (Fig. 2). Data are ranked in ascending order. A detailed list of the phenolics and their fold-change values are reported in Tab. S5.

Considering the 10 min UV-B exposure, 103 (57%) phenolic compounds were found to accumulate 36 h after the treatment in comparison to the 24-h recovery time, while only 77 (43%) decreased. However, in the 60 min UV-B treated fruit, almost all the phenolics (89%) underwent an increase 36 h after the exposure, suggesting a stronger effect of the 60 min compared to the 10 min UV-B treatment. Furthermore, while in the 10 min irradiated samples the lowest concentrated phenolic had a fold-change value of −3.6, in the 60 min irradiated fruit the lowest fold-change was −1.5. This means that the 60 min UV-B treatment not only determined a higher number of increased phenolics, but also that the decreased ones underwent a minor reduction, revealing the effectiveness of a longer UV-B exposure in stimulating the phenolic metabolism.

The fold-change analysis (24 h vs 36 h) clearly highlighted an accumulation of most phenolics after 36 h when compared to the 24 h, in both the UV-B treatments, suggesting a UV-B-triggered upregulation of flavonoid-related genes.

3.3. Gene expression patterns

3.3.1. UVR8 pathway-related genes

All is known about UV-B perception and signalling mainly derives from studies carried out in *Arabidopsis* and very few papers have been published about UVR8 signalling in fruit. Accordingly, some genes related to the UVR8 pathway, particularly *PpUVR8*, *PpCOP1* and *PpHY5* (Fig. 3), have been investigated in UV-B exposed skin of peach fruit to determine whether the UV-B perception and signalling cascade were similar to those described in *Arabidopsis*.

PpUVR8 expression pattern in the both UV-B-treated fruit was not significantly different to the control, although a slightly higher transcript abundance was detectable 6 h after both the UV-B exposures ($P = 0.2097$ for 6 h; $P = 0.9439$ for 12 h; $P = 0.9327$ for 24 h; $P = 0.3882$ for 36 h).

On the contrary, *PpCOP1* gene was found to be strongly and significantly responsive to UV-B radiation. While under control condition *PpCOP1* expression showed a steady trend of decline, a significant increase in the UV-B exposed skin was found at 6 h and 24 h after the onset of the 60 min UV-B treatments. Moreover, the peaches treated with 60 min UV-B also showed a higher transcript abundance 12 h after the exposure compared to the 10 min-UVB-treated peaches.

Similar to *PpCOP1*, also *PpHY5* transcription was significantly affected by UV-B. *PpHY5* expression of the UV-B-exposed samples displayed a significant increase at 6 h and 24 h time points compared to the control. Differences among the two treatments were significant only

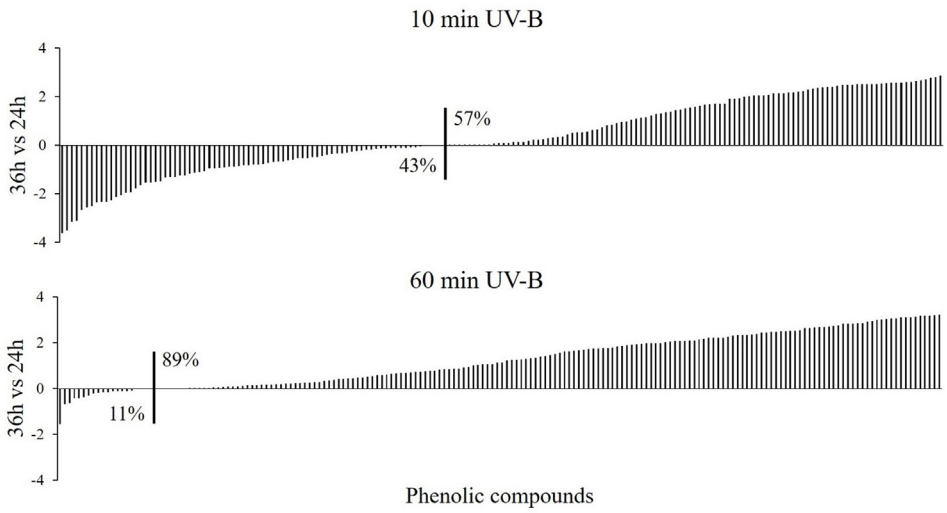

Fig. 2. Fold-change (36 h vs 24 h) of phenolics accumulation considering each UV-B treatment (10 min and 60 min, 1.39 kJ m^{-2} and 8.33 kJ m^{-2} UV-B, respectively). Each bar represents a single phenolic compound. Percentages in each plot refer to the number of phenolic compounds undergoing a decrease (left) or an increase (right) after 36 h in respect to the 24 h timepoint. Detailed list of the phenolics and their fold-change values are reported in Tab. S5.

after 6 h from the UV-B irradiation, where the 10 min- UV-B samples showed a higher transcript level than the 60 min-UVB ones.

A previous study in *Arabidopsis* observed that the transcript abundance of *AtCOP1* gene progressively increased together with a higher UV-B dose (Huang et al., 2012), confirming the UV-B-induced transcription of *COP1*. Considering *HY5* gene, studies highlighted that its transcription in *Arabidopsis* is induced by UV-B radiation (Brown and Jenkins, 2007).

Recently, UVR8 orthologues have been isolated and functionally characterised in apple (Zhao et al., 2016) and grapevine (UVR1), where HY5 and HYH orthologues and their putative targets have been also isolated (Loyola et al., 2016). The increased transcription of both *PpCOP1* and *PpHY5* in UV-B-treated samples suggests the presence of a mechanism of UV-B perception and signalling similar to that described in *Arabidopsis* also in peach fruit. Interestingly, both *PpCOP1* and *PpHY5* exhibited a biphasic kinetic of activation, similar to the well-known behaviour of ROS, ethylene, salicylic acid and other molecules in response to biotic and abiotic stresses (Wi et al., 2012), that would allow amplification of the signal. Contrarily to the previous genes tested, *PpUVR8* gene expression did not display any upregulation. This result is in accordance with a previous study (Rizzini et al., 2011), which showed that UVR8 protein is constitutively expressed within the cell. In fact, since plants must promptly trigger defensive mechanisms against potentially damaging UV-B radiation, the presence of pre-formed UVR8 dimers might be an evolutionary tract to adopt quick adaptations in response to UV-B radiation. Consistently, it was found in literature that both in *Arabidopsis* (Kaiserli and Jenkins, 2007) and in Sauvignon grape berry (Liu et al., 2014) the *UVR8* transcript level does not differ in relation to different light quality. Our results revealed an “up and down” trend, with the higher expression 24 h after the UV-B exposure, in all the samples. These fluctuations might represent physiological changes occurring during ripening of the fruit. In fact, variations in *MdUVR8* expression level were observed during development in preharvest apple when solar UV-B and UV-A were depleted (Henry-Kirk et al., 2018).

3.3.2. Phenylpropanoid biosynthetic genes

The influence of UV-B exposure on the flavonoid biosynthetic pathway in peach peel was checked by measuring expression of some biosynthetic genes (*PpCHS*, *PpF3H*, *PpF3′H* and *PpDFR*) (Fig. 3).

Transcript levels of *PpCHS*, a very early gene in flavonoid pathway, showed a strong increase in UV-B exposed skin 6 h after the 60 min UV-B treatment. Although not significant, also the 10 min UV-B exposure showed a trend to increase after 6 h from the irradiation. However, in later time points, the transcript abundance of the 60-min UV-B treated peaches was the same as the control. Contrarily, *PpCHS* expression level in the 10-min UV-B exposed ones remained significantly higher considering the 24 h and 36 h recovery times. Regarding *PpF3H*, a marked increase in its transcript level was detected in the 60min-6h sample, while, after 24 h, the 10-min UV-B exposed peaches showed a significantly higher *PpF3H* expression compared to both control and the 60 min UV-B treated samples.

PpF3′H showed a different behaviour, displaying a slight decrease in the storage period in relation to control samples. The 10-min UV-B treated samples, however, did not decrease immediately as for the control. Their expression level decreased later than control, after 6 h, but then the transcript increased at the 24 h-time point and it was maintained in a steady state up to 36 h. The 60-min UV-B exposed fruit behaved similarly to the control, with the difference that an increase in expression was detected 24 h after exposure.

Finally, the *PpDFR* gene expression pattern was generally similar between the UV-B treated samples and the control, with the exception that the 60-min exposed peaches showed a strong UV-B induced upregulation 6 h after the treatment. However, the *PpDFR* transcript abundance returned to control level from 12 h until the end of the recovery period considered.

An upregulation of *PpCHS* gene was observed in two peach cultivars, Suncrest and Big Top, after postharvest UV-B exposure (36 h) (Scattino et al., 2014). In two other peach cultivars, Hujingmilu and Yulu, a 2-days-postharvest UV-B treatment (58 mW/cm^2) induced an upregulation of several genes involved in flavonoid biosynthesis, such as *PpCHS*, *PpF3H*, *PpF3′H* and *PpDFR,* together with an accumulation of anthocyanins (Zhao et al., 2017). Similar results were obtained also with other fruit. An increase of *MdCHS* transcription was detected in the skin of five apple cultivars subjected to a 5 days-postharvest UV-B treatment at 17 °C (Ubi et al., 2006). In tomato, it was observed that shielding UV-B radiation during ripening resulted in a reduced *LeCHS* transcription (Catola et al., 2017). Similarly to *CHS* gene, it was found a more abundant *MdF3H* transcript in apple skin, suggesting a probable involvement of F3H in UV-B acclimation (Ubi et al., 2006).

The UV-B triggered activation of *DFR* gene was reported also in apple skin exposed to UV-B radiation (Ubi et al., 2006).

The UV-B-induced activation of such phenylpropanoid biosynthetic genes correlates to the fluctuation observed in phenolics content. A hypothetical scenario of possible events occurring in peach skin is depicted in Fig. 4. The decrease of total phenolic content detected 24 h after both UV-B treatments, but particularly for the 60-min exposed samples, suggests that UV-B might have triggered an oxidative stress in the irradiated peach skin. Such hypothetical oxidative stress might have induced a reduction in the phenolic content, due to their consumption

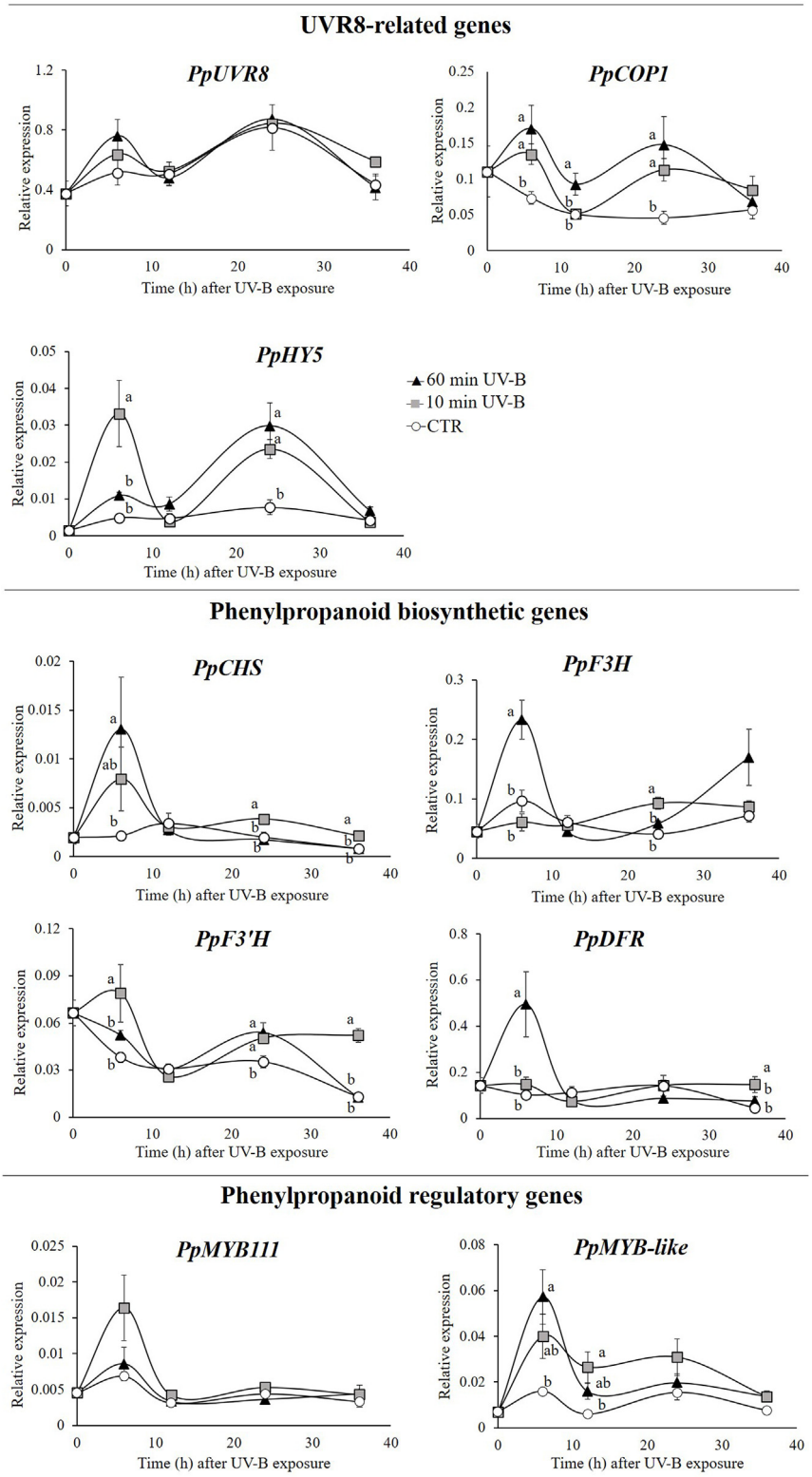

Fig. 3. Effect of UV-B exposure on transcript abundance of several genes involved in UVR8 pathway (*UVR8*, *COP1*, *HY5*), and in phenylpropanoid pathway (*CHS*, *F3H*, *F3′H*, *DFR*, *MYB111*, *MYB-like*) in peach skin. CTR refers to control samples (untreated with UV-B). Data are mean ± SE of five biological replicates. Different letters correspond to statistically significant differences according to one-way ANOVA followed by Tukey–Kramer post hoc test ($P \leq 0.05$).

to counteract the UV-B-induced ROS. Simultaneously, since UV-B radiation also triggers specific UVR8-mediated intracellular responses leading to the acclimation to ambient UV-B condition, newly-synthesized phenolic compounds start to accumulate, visible 36 h after UV-B irradiation, via the upregulation of several flavonoid regulatory and biosynthetic genes. RT-qPCR analysis confirmed the UV-B-triggered activation of the UVR8 pathway, as well as the stimulation of most of the phenylpropanoid-related genes investigated. Confirmation of such hypothesis requires validation experiments on ROS production and scavenging by enzymatic and non-enzymatic systems within peach skin

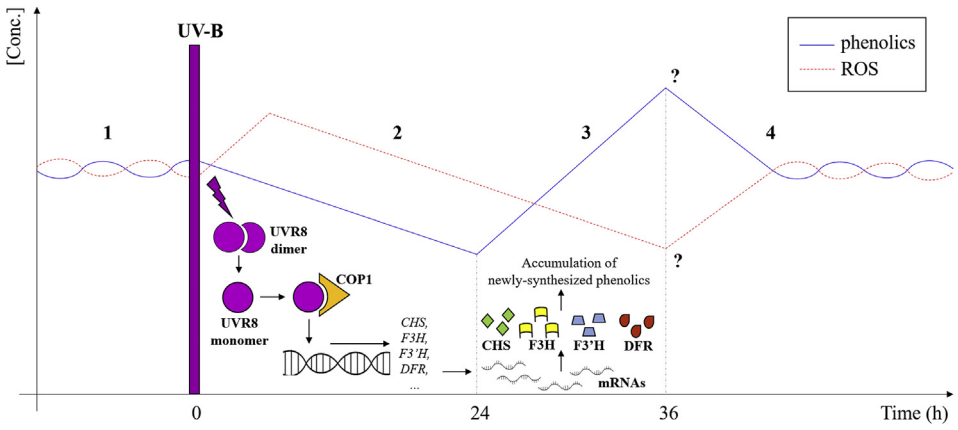

Fig. 4. Hypothetical behaviour of UV-B-induced ROS based on both the molecular and biochemical results presented in this study. Before the UV-B treatment and without additional sources of stress, phenolics and ROS are balanced, with few fluctuations due to the physiological processes within the cell (1). When fruit are UV-B-irradiated, ROS immediately increase, but then they are promptly neutralized by phenolic compounds, which start to be consumed to counteract the harmful effects of UV-B induced ROS (2). However, as an acclimation response, UV-B triggers the activation of several phenolics-related genes via UVR8 pathway. The resulting increase of phenolics biosynthetic enzymes determined an accumulation of phenolic compounds (3), which were visible 36 h after the irradiation. For longer timepoints, since UV-B radiation is not present anymore, it is likely that the UV-B signal is suppressed, thus both the phenolics and ROS levels are restored to the physiological initial concentration (4).

under the UV-B doses tested.

3.3.3. MYB-transcription factors involved in the phenylpropanoid biosynthesis

R2R3 MYB transcription factors have been shown to play essential roles in regulation of UV-B stimulated expression of phenylpropanoid biosynthesis genes (Falcone Ferreyra et al., 2012). A homolog of MYB111 have been shown already to be significantly induced by UV-B in peels of nectarines (Ravaglia et al., 2013). A screen for genes induced between the 8th and 10th week after full bloom of the peaches the *MYB-like* gene (a homolog of the *Arabidopsis AtMYB110* and *AtMYB105*) was identified through microarray expression (Guidarelli et al., 2014).

The *PpMYB111* was significantly UV-B-induced in the 10 min UV-B treated samples after 6 h while at later time points the expression resembled that of control and the 60 min treatment.

As observed in most of previous genes, the *PpMYB-like* gene displayed a significant upregulation at 6 h after the onset of the 60 min UV-B treatments, while at later time points the expression decreased and was only in the 10 min samples significantly higher than in control and the 60 min treatment.

Previous works reported that PpMYB10.1 and PpMYB10.3 are the main responsible for anthocyanin biosynthesis in peach fruit (Tuan et al., 2015). In grapevine, it was found that the R2R3-MYB *VvMYBF1* is involved in the expression of *VvFLS* gene, thus inducing synthesis of several flavonols (Czemmel et al., 2017). The same study found a correlation between overexpression of *VvMYBF1* and the modulation of the UV-B-induced transcription factor HY5. Involvement of different environmental stresses-induced R2R3 MYB members in regulating several flavonoid subclasses, such as flavonols and anthocyanins, has been reported in many other plant species (Cao et al., 2017; Shin et al., 2016). In our study, the UV-B-triggered expression of two MYB transcription factors, PpMYB111 and PpMYB-like, has been investigated in peach skin.

MYB111 was found to be a positive regulator for several flavonoid biosynthetic genes involved in the early stages of flavonoid synthesis in *Arabidopsis*, such as *AtCHS*, *AtCHI*, *AtF3H* (Pandey et al., 2014). MYB111, together with its homologues MYB11 and MYB12 which share target flavonoid gene specificity, has been found to promote flavonols accumulation in transgenic tobacco, but light was observed to be necessary for stimulating flavonoid biosynthesis by MYBs (Zhou et al., 2017).

4. Conclusions

Several studies investigated the effect of UV-B radiation on plants. However, the literature on molecular and biochemical effects of postharvest UV-B treatments, as well as the presence of a UV-B perception mechanism in fruit, is scarce. In this work, an "-omics" approach was adopted to investigate the influence of UV-B radiation on the phenolic profile of peach skin, combining the metabolomic data with gene expression analyses. Our study revealed that the UV-B treatments activate genes involved in both UVR8 signalling and phenylpropanoid biosynthesis. Therefore, several phenolic compounds such as anthocyanins, after an early decrease probably due to their role as ROS scavengers, accumulated 36 h after the UV-B exposure, mainly in the 60 min UV-B irradiated samples. Although preliminary, this study exemplifies the possible exploitation of UV-B treatment as an eco-friendly tool to improve the quality of peaches after harvesting. However, the results of this research, despite the use of five biological replicates, derive from an un-replicated UV-B irradiation, thus caution should be adopted in drawing general conclusions. In this sense, further studies are necessary, also to determine cultivar specific differences towards UV-B. Moreover, since we found a UV-B-induced modulation of specific phenolic subclasses without an overall increase in total phenolic content, additional research is advised to find UV-B dose(s) able to promote total phenolic accumulation. Similarly, correlating phenolics to other UV-B specific fruit characteristics (e.g. skin color, ripening period, melting phenotype, etc.) might help to uncover the most effective treatment for applicative use of postharvest UV-B radiation.

CRediT authorship contribution statement

Marco Santin: Investigation, Data curation, Writing – original draft, Writing – review & editing. **Luigi Lucini:** Investigation, Writing – review & editing. **Antonella Castagna:** Data curation, Writing – review & editing. **Gabriele Rocchetti:** Investigation, Data curation, Writing – original draft, Writing – review & editing. **Marie-Theres Hauser:** Conceptualization, Funding acquisition, Supervision, Data curation, Writing – review & editing. **Annamaria Ranieri:** Conceptualization, Funding acquisition, Supervision, Writing – review & editing.

Acknowledgements

The research was supported by funds of the University of Pisa. MS conducted part of the study in the laboratory of M.T.H. at the Department of Applied Genetics and Cell Biology, University of Natural Resources and Life Sciences which was supported by a grant of the Austrian Science Fund FWF I 1725-B16. We kindly acknowledge the technical support of Julia Richter and Nataliia Konstantinova for help with the sampling. MS was further supported by an Erasmus + traineeship.

Appendix A. Supplementary data

Supplementary data to this article can be found online at https://doi.org/10.1016/j.plaphy.2018.11.009.

References

Altschul, S.F., Madden, T.L., Schäffer, A.A., Zhang, J., Zhang, Z., Miller, W., Lipman, D.J., 1997. Gapped BLAST and PSI-BLAST:a new generation of protein database search programs. Nucleic Acids Res. 25, 3389–3402. https://doi.org/10.1093/nar/25.17.3389.

Assumpção, C.F., Hermes, V.S., Pagno, C., Castagna, A., Mannucci, A., Sgherri, C., Pinzino, C., Ranieri, A., Flôres, S.H., Rios, A. de O., 2018. Phenolic enrichment in apple skin following post-harvest fruit UV-B treatment. Postharvest Biol. Technol. 138, 37–45. https://doi.org/10.1016/j.postharvbio.2017.12.010.

Bartel, J., Krumsiek, J., Theis, F.J., 2013. Statistical methods for the analysis of high-throughput metabolomics data. Comput. Struct. Biotechnol. J. 4, e201301009. https://doi.org/10.5936/csbj.201301009.

Brown, B.A., Cloix, C., Jiang, G.H., Kaiserli, E., Herzyk, P., Kliebenstein, D.J., Jenkins, G.I., 2005. A UV-B-specific signaling component orchestrates plant UV protection. Proc. Natl. Acad. Sci. U. S. A 102, 18225–18230. https://doi.org/10.1073/pnas.0507187102.

Brown, B.A., Jenkins, G.I., 2007. UV-B signaling pathways with different fluence-rate response profiles are distinguished in mature arabidopsis leaf tissue by requirement for UVR8, HY5, and HYH. Plant Physiol. 146, 576–588. https://doi.org/10.1104/pp.107.108456.

Cao, X., Qiu, Z., Wang, X., Van Giang, T., Liu, X., Wang, J., Wang, X., Gao, J., Guo, Y., Du, Y., Wang, G., Huang, Z., 2017. A putative R3 MYB repressor is the candidate gene underlying atroviolacium, a locus for anthocyanin pigmentation in tomato fruit. J. Exp. Bot. 68, 5745–5758. https://doi.org/10.1093/jxb/erx382.

Catola, S., Castagna, A., Santin, M., Calvenzani, V., Petroni, K., Mazzucato, A., Ranieri, A., 2017. The dominant allele Aft induces a shift from flavonol to anthocyanin production in response to UV-B radiation in tomato fruit. Planta 246, 263–275. https://doi.org/10.1007/s00425-017-2710-z.

Cloix, C., Kaiserli, E., Heilmann, M., Baxter, K.J., Brown, B.A., O'Hara, A., Smith, B.O., Christie, J.M., Jenkins, G.I., 2012. C-terminal region of the UV-B photoreceptor UVR8 initiates signaling through interaction with the COP1 protein. Proc. Natl. Acad. Sci. Unit. States Am. 109, 16366–16370. https://doi.org/10.1073/pnas.1210898109.

Czemmel, S., Höll, J., Loyola, R., Arce-Johnson, P., Alcalde, J.A., Matus, J.T., Bogs, J., 2017. Transcriptome-wide identification of novel UV-B- and light modulated flavonol pathway genes controlled by VviMYBF1. Front. Plant Sci. 8, 1–15. https://doi.org/10.3389/fpls.2017.01084.

Falcone Ferreyra, M.L., Rius, S.P., Casati, P., Hellmann, H.A., Roje, S., Goyer, A., de Estudios Fotosintéticos Bioquímicos, C., 2012. Flavonoids: biosynthesis, biological functions, and biotechnological applications. https://doi.org/10.3389/fpls.2012.00222.

Favory, J.J., Stec, A., Gruber, H., Rizzini, L., Oravecz, A., Funk, M., Albert, A., Cloix, C., Jenkins, G.I., Oakeley, E.J., Seidlitz, H.K., Nagy, F., Ulm, R., 2009. Interaction of COP1 and UVR8 regulates UV-B-induced photomorphogenesis and stress acclimation in Arabidopsis. EMBO J. 28, 591–601. https://doi.org/10.1038/emboj.2009.4.

Frohnmeyer, H., 2003. Ultraviolet-B radiation-mediated responses in plants. Balancing damage and protection. Plant Physiol. 133, 1420–1428. https://doi.org/10.1104/pp.103.030049.

Guidarelli, M., Zubini, P., Nanni, V., Bonghi, C., Rasori, A., Bertolini, P., Baraldi, E., 2014. Gene expression analysis of peach fruit at different growth stages and with different susceptibility to Monilinia laxa. Eur. J. Plant Pathol. 140, 503–513. https://doi.org/10.1007/s10658-014-0484-8.

Henry-Kirk, R.A., Plunkett, B., Hall, M., McGhie, T., Allan, A.C., Wargent, J.J., Espley, R.V., 2018. Solar UV light regulates flavonoid metabolism in apple (Malus x domestica). Plant Cell Environ. 675–688. https://doi.org/10.1111/pce.13125.

Huang, X., Ouyang, X., Yang, P., Lau, O.S., Li, G., Li, J., Chen, H., Deng, X.W., 2012. Arabidopsis FHY3 and HY5 positively mediate induction of COP1 transcription in response to photomorphogenic UV-B light. Plant Cell 24, 4590–4606. https://doi.org/10.1105/tpc.112.103994.

Jenkins, G.I., 2014. Structure and function of the UV-B photoreceptor UVR8 This review comes from a themed issue on Multi-protein assemblies in signalling. Curr. Opin. Struct. Biol. 29, 52–57. https://doi.org/10.1016/j.sbi.2014.09.004.

Kaiserli, E., Jenkins, G.I., 2007. UV-B promotes rapid nuclear translocation of the arabidopsis UV-B specific signaling component UVR8 and activates its function in the nucleus. Plant Cell 19, 2662–2673. https://doi.org/10.1105/tpc.107.053330.

Karsai, A., Müller, S., Platz, S., Hauser, M.T., 2002. Evaluation of a home-made SYBR® Green I reaction mixture for real-time PCR quantification of gene expression. Biotechniques 32, 790–796.

Liu, Y., Li, D., Zhang, Y., Sun, R., Xia, M., 2014. Anthocyanin Increases Adiponectin Secretion and Protects against Diabetes-related Endothelial Dysfunction, vol. 2. pp. 975–988. https://doi.org/10.1152/ajpendo.00699.2013.

Loyola, R., Herrera, D., Mas, A., Wong, D.C.J., Höll, J., Cavallini, E., Amato, A., Azuma, A., Ziegler, T., Aquea, F., Castellarin, S.D., Bogs, J., Tornielli, G.B., Peña-Neira, A., Czemmel, S., Alcalde, J.A., Matus, J.T., Arce-Johnson, P., 2016. The photomorphogenic factors UV-B RECEPTOR 1, ELONGATED HYPOCOTYL 5, and HY5 HOMOLOGUE are part of the UV-B signalling pathway in grapevine and mediate flavonol accumulation in response to the environment. J. Exp. Bot. 67, 5429–5445. https://doi.org/10.1093/jxb/erw307.

Pandey, A., Misra, P., Bhambhani, S., Bhatia, C., Trivedi, P.K., 2014. Expression of arabidopsis myb transcription factor, atmyb111, in tobacco requires light to modulate flavonol content. Sci. Rep. 4. https://doi.org/10.1038/srep05018.

Ravaglia, D., Espley, R. V, Henry-kirk, R.A., Andreotti, C., Ziosi, V., Hellens, R.P., Costa, G., Allan, A.C., 2013. art%3A10.1186%2F1471-2229-13-68.

Richter, J., Ploderer, M., Mongelard, G., Gutierrez, L., Hauser, M.-T., 2017. Role of CrRLK1L cell wall sensors HERCULES1 and 2, THESEUS1, and FERONIA in growth adaptation triggered by heavy metals and trace elements. Front. Plant Sci. 8, 1–12. https://doi.org/10.3389/fpls.2017.01554.

Rizzini, L., Favory, J.J., Cloix, C., Faggionato, D., O'Hara, A., Kaiserli, E., Baumeister, R., Schäfer, E., Nagy, F., Jenkins, G.I., Ulm, R., 2011. Perception of UV-B by the arabidopsis UVR8 protein. Science (Washington, D.C.) 332, 103–106. https://doi.org/10.1126/science.1200660.

Rocchetti, G., Chiodelli, G., Giuberti, G., Ghisoni, S., Baccolo, G., Blasi, F., Montesano, D., Trevisan, M., Lucini, L., 2018. UHPLC-ESI-QTOF-MS profile of polyphenols in Goji berries (Lycium barbarum L.) and its dynamics during in vitro gastrointestinal digestion and fermentation. J. Funct. Foods 40, 564–572. https://doi.org/10.1016/j.jff.2017.11.042.

Rothwell, J.A., Perez-Jimenez, J., Neveu, V., Medina-Remón, A., M'Hiri, N., García-Lobato, P., Manach, C., Knox, C., Eisner, R., Wishart, D.S., Scalbert, A., 2013. Phenol-Explorer 3.0: a major update of the Phenol-Explorer database to incorporate data on the effects of food processing on polyphenol content. Database 2013, 1–8. https://doi.org/10.1093/database/bat070.

Santin, M., Lucini, L., Castagna, A., Chiodelli, G., Hauser, M., Ranieri, A., 2018. Post-harvest UV-B radiation modulates metabolite profile in peach fruit. Postharvest Biol. Technol. 139, 127–134. https://doi.org/S0925521417309171.

Scattino, C., Castagna, A., Neugart, S., Chan, H.M., Schreiner, M., Crisosto, C.H., Tonutti, P., Ranieri, A., 2014. Post-harvest UV-B irradiation induces changes of phenol contents and corresponding biosynthetic gene expression in peaches and nectarines. Food Chem. 163, 51–60. https://doi.org/10.1016/j.foodchem.2014.04.077.

Schreiner, M., Martínez-Abaigar, J., Glaab, J., Jansen, M., 2014. UV-B Induced Secondary Plant Metabolites. Opt. Photonik 9, 34–37. https://doi.org/10.1002/opph.201400048.

Shin, D.H., Choi, M.G., Kang, C.S., Park, C.S., Choi, S.B., Park, Y. Il, 2016. A wheat R2R3-MYB protein PURPLE PLANT1 (TaPL1) functions as a positive regulator of anthocyanin biosynthesis. Biochem. Biophys. Res. Commun. 469, 686–691. https://doi.org/10.1016/j.bbrc.2015.12.001.

Tuan, P.A., Bai, S., Yaegaki, H., Tamura, T., Hihara, S., Moriguchi, T., Oda, K., 2015. The crucial role of PpMYB10.1 in anthocyanin accumulation in peach and relationships between its allelic type and skin color phenotype. BMC Plant Biol. 15, 1–14. https://doi.org/10.1186/s12870-015-0664-5.

Ubi, B.E., Honda, C., Bessho, H., Kondo, S., Wada, M., Kobayashi, S., Moriguchi, T., 2006. Expression analysis of anthocyanin biosynthetic genes in apple skin: effect of UV-B and temperature. Plant Sci. 170, 571–578. https://doi.org/10.1016/j.plantsci.2005.10.009.

Wi, S.J., Ji, N.R., Park, K.Y., 2012. Synergistic biosynthesis of biphasic ethylene and reactive oxygen species in response to hemibiotrophic phytophthora parasitica in tobacco plants. Plant Physiol. 159, 251–265. https://doi.org/10.1104/pp.112.194654.

Worley, B., Powers, R., 2012. Multivariate analysis in metabolomics. Curr. Metabolomics 1, 92–107. https://doi.org/10.2174/2213235X11301010092.

Zhang, C., Tian, S., 2009. Crucial contribution of membrane lipids' unsaturation to acquisition of chilling-tolerance in peach fruit stored at 0 °S{cyrillic}. Food Chem. 115, 405–411. https://doi.org/10.1016/j.foodchem.2008.12.021.

Zhao, C., Mao, K., You, C.X., Zhao, X.Y., Wang, S.H., Li, Y.Y., Hao, Y.J., 2016. Molecular cloning and functional analysis of a UV-B photoreceptor gene, MdUVR8 (UV Resistance Locus 8), from apple. Plant Sci. 247, 115–126. https://doi.org/10.1016/j.plantsci.2016.03.006.

Zhao, Y., Dong, W., Wang, K., Zhang, B., Allan, A.C., Lin-wang, K., Chen, K., Xu, C., 2017. Differential sensitivity of fruit pigmentation to ultraviolet light between two. Peach Cultivars 8, 1–15. https://doi.org/10.3389/fpls.2017.01552.

Zhou, Z., Schenke, D., Miao, Y., Cai, D., 2017. Investigation of the crosstalk between the flg22 and the UV-B-induced flavonol pathway in Arabidopsis thaliana seedlings. Plant Cell Environ. 40, 453–458. https://doi.org/10.1111/pce.12869.